Journal of Molecular Catalysis A: Chemical 318 (2010) 15–20

Contents lists available at ScienceDirect

Journal of Molecular Catalysis A: Chemical

journal homepage: www.elsevier.com/locate/molcata

Influence of the preparation methods and redox properties of $Cu/ZnO/Al_2O_3$ catalysts for the water gas shift reaction

Renan Tavares Figueiredo[a,*], Heloysa Martins Carvalho Andrade[b], José L.G. Fierro[c]

[a] Instituto de Tecnología e Pesquisa - Universidade Tiradentes-ITP/UNIT, Av. Murilo Dantas, 300, 49030-270 Aracajú - SE, Brazil
[b] Instituto de Química, Universidade Federal da Bahia, Campus Universitário de Ondina s/n, 40170-290 Salvador - BA, Brazil
[c] Instituto de Catálisis y Petroleoquímica, CSIC, Cantoblanco, 28049 Madrid, Spain

ARTICLE INFO

Article history:
Received 25 August 2009
Received in revised form 23 October 2009
Accepted 27 October 2009
Available online 6 November 2009

Keywords:
LT-WGSR
Cu/Zn/Al catalysts
Copper dispersion
Reduction
Oxidation

ABSTRACT

Different coprecipitation sequences were used to prepare $Cu/ZnO/Al_2O_3$ catalysts for the water gas shift reaction. The interdispersion of the components of the obtained mixture of hydroxycarbonates seemed to be influenced by the coprecipitation sequence, at constant pH and temperature. High metallic copper surface area was observed when Cu^{2+} and Zn^{2+} ions were simultaneously coprecipitated. A remarkable activity was found to be related to the catalyst ability to restore the copper surface dispersion after reduction or oxidation pre-treatment. These last findings were evidenced by temperature-programmed reduction and X-ray photoelectron spectroscopy experiments.

1. Introduction

Copper/zinc oxide/alumina catalysts are successfully used for the low temperature water gas shift reaction (LT-WGSR) in industrial ammonia plants. They allow an efficient carbon monoxide removal, achieving exit concentration as low as 0.1–0.3%, which is a pre-requisite for the subsequent steps in the synthesis process [1]. As this is of economic concern, much attention has been paid to the understanding of the underlining catalytic chemistry and the role of each catalyst component [2–7].

The oxide precursors are commonly obtained from hydroxycarbonate mixtures prepared by coprecipitation. However, despite the great effort to rationalize the effects of the preparation conditions on the final catalyst, these results are frequently evasive and scarcely generalized [7–10]. For instance, Li and Inui [11] have found that the pH alters the phase composition and that the temperature affects the precipitation kinetics of the catalytic precursors, while the aging temperature determines phase interdispersion. On the other hand, finely dispersed metallic copper supported on ZnO or $ZnO–Al_2O_3$ phases is currently accepted to be the active phase and the catalytic activity to be proportional to the metallic surface area of copper. However, there still remains some controversy about the actual oxidation state of copper under reaction conditions [12,13].

Yurieva [14] considered that the catalytic properties of highly dispersed oxide mixtures of copper and zinc (with or without alumina) are determined in two stages, namely, the preparation of the oxide mixture and the catalyst activation by reduction of the oxides. Thus, an active LT-WGSR catalyst should present high phase interdispersion and enhanced redox properties.

In order to further contribute to the understanding of the chemistry of $Cu/ZnO/Al_2O_3$ catalyst, the surface composition of ternary Cu–Zn–Al (40–45–15) catalyst precursors was investigated under a reduction–oxidation cycle. The catalysts were prepared following different coprecipitation sequences but at constant experimental conditions. The main physico-chemical characteristics of the catalysts after reduction and oxidation treatments were analyzed in terms of their activity towards the low temperature–water gas shift reaction. It has been observed that the precipitation sequence affects the interdispersion and the stability of the copper containing surface phases, thus determining the catalytic activity for LT-WGSR.

2. Experimental

2.1. Preparation of catalyst precursors

Analytical grade chemicals were used for the preparations. Three different procedures were employed in catalyst preparation: (i) catalyst CZA: in this case, the Cu^{2+}, Zn^{2+} and Al^{3+} ions were simultaneously precipitated from nitrate solutions (0.5 M), using a Na_2CO_3 solution (0.3 M), at 343 K. The suspension was stirred for

* Corresponding author. Tel.: +55 079 3218 2190; fax: +55 079 3218 2190.
E-mail address: renantf@infonet.com.br (R.T. Figueiredo).

1381-1169/$ – see front matter © 2009 Elsevier B.V. All rights reserved.
doi:10.1016/j.molcata.2009.10.028

1 h and cooled under stirring for 1 h. The final pH was 7.8–8.0. After washing with deionized water, at 343 K, up to 0.2 ppm [Na], the solid was dried at 383 K, for 12 h and calcined at 773 K, for 4 h. (ii) Catalyst CZ-A: in this case, the Cu^{2+}, Zn^{2+} ions were coprecipitated from nitrate solutions (0.5 M), using a Na_2CO_3 solution (0.3 M), at 343 K and then mixed with the Al^{3+} hydroxycarbonate that was precipitated separately. Thereafter, the preparation followed the previously described procedure (i). (iii) Catalyst CA-Z: in this case, the Cu^{2+}, Al^{3+} ions were coprecipitated from nitrate solutions (0.5 M), using a Na_2CO_3 solution (0.3 M), at 343 K and then mixed with the Zn^{2+} hydroxycarbonate that was precipitated separately. Thereafter, the preparation followed the previously described procedure (i).

2.2. Characterization techniques

The chemical composition of the samples was determined by inductively coupled plasma adsorption spectrometry using an ARL ICP-OES equipment, model 3410. The specific surface area was calculated according to the BET method from the nitrogen adsorption isotherms recorded at 77 K (CG 2000 A equipment) on samples degassed overnight at 573 K. The pore volumes were determined on a Micromeritics Pore Sizer 9305. Copper metallic surface area and dispersion were determined using the dissociative chemisorptions of nitrous oxide (N_2O) and the frontal method [8]. The X-ray diffraction spectra were obtained with a Philips-Norelco diffractometer with nickel-filtered Cu Kα radiation and a graphite secondary bean monochromator. The intensities were obtained in the 2 theta ranges between 20 and 90° with a step of 0.05° and a measuring time of 0.5 s per point. FTIR spectra of the catalyst precursors were collected on a Jasco, Valor III spectrometer, using KBr pellets. TPR measurements were carried out in an automatic Micromeritics 3000 apparatus, using 30 mg of the calcined sample, heating rate β = 4 K/min, from 290 to 750 K, in a 80 ml/min flow of 10% H_2/N_2.

X-ray photoelectron spectra were recorded with a VG 200 R electron spectrometer operated in a constant pass mode and provided with a non-monochromatized MgKα ($h\nu$ = 1253.6 eV, 1 eV = 1.603×10^9 J) X-ray source operated at 10 mA and 12 kV. Prior to analysis the samples were pretreated in the treatment chamber of the spectrometer according to the following protocols. The precursors were firstly subjected to oxidation (673 K, in air flow, for 2 h) and then to reduction (493 K, in H_2 flow, for 1 h). The catalysts were analyzed after each step of the following cycle: (i) calcination; (ii) reduction; (iii) oxidation; (iv) reduction. The pressure in the ion-pumped chamber was below 3×10^{-9} Torr during data acquisition. The Cu 2p; Zn 2p; Al 2p; O 1s and C 1s energy regions were recorded for each sample and the respective binding energies (BE) were calibrated using the C 1s line at 284.9 eV as internal reference. BE values within an accuracy of 0.2 eV were obtained. Data processing was performed with the *XPS peak* program. The spectra were decomposed with the least squares fitting routine provided with the software, with a Gauss/Lorentz product function and after subtracting a Shirley background. High resolution spectra envelopes were obtained by curve fitting synthetic peak components using the software "*XPS peak*". The raw data were used with no preliminary smoothing. Symmetric Gaussian–Lorentzian product functions were used to approximate the line shapes of the fitting components. Atomic ratios were computed from experimental intensity ratios and normalized by atomic sensitivity factors [15].

2.3. Catalyst testing

Activity measurements were carried out using a fixed bed tubular reactor consisting of a 40 cm stainless steel tube (i.d. 1.3 cm), operated at atmospheric pressure. A washing flask containing sulfuric acid was used to remove water from the exit gases. The feed gas of volumetric composition 0.25% CH_4; 16.5% CO_2; 3.2% CO; 0.2% Ar; 20.5% N_2 and 59.3% H_2, was supplied from an industrial ammonia plant. Steam was supplied to the reactor from a saturator containing distilled water, under rigorous temperature control, in order to allow an accurate variation of the vapor/gas (V/G) molar ratio. The space velocity was 4.500 h^{-1} during the reaction tests. The reaction conditions for activity testing were established in order to avoid mass transfer limitations. The feed gas and reaction effluents were analyzed using a Hewlett-Packard HP5890 gas chromatograph, with a thermal conductivity detector and a 13X molecular sieve column. CO_2 was separately analyzed using a Porapak Q column. 0.05–0.10 g of powdered (−100/+150 mesh) catalyst samples were activated *in situ*, heating up to 393 K in N_2 flow and then up to 493 K, using a 7.5% H_2/N_2 reducing mixture, at 4 K/min. Before testing, the catalyst was reduced for further 2 h at 493 K and 4.500 h^{-1} space velocity.

Table 1
Composition and characterization of the catalysts.

Property/catalyst	CZA	CZ-A	CA-Z	Commercial
% CuO	38	39	39	35
% ZnO	43	45	44	45
% Al_2O_3	19	16	17	20
V_p (ml/g)	0.56	0.79	1.0	0.30
S_{BET} (m^2/g)	90.5	100.4	78.4	53.4
S_{cu} (m^2/g)	25.3	61.3	18.9	39.3
% D	5.7	13.8	4.3	8.9

3. Results and discussion

3.1. Preparation and characterization

The main physico-chemical properties of the obtained catalysts are shown in Table 1. A commercial catalyst sample has also been also included as a source of comparison. The chemical analyses revealed that the catalyst bulk compositions were nearly constant, irrespective of the coprecipitation sequence. The obtained precursors were analyzed by XRD and FTIR. These techniques indicated that the precursors contain a mixture of hydroxycarbonates. Major phases identified included: rosasite [$(Cu,Zn)_2CO_3(OH)_2$], hydrotalcite [$(Cu,Zn)_6Al_2CO_3(OH)_{16}\cdot H_2O$] and aurichalcite [$(Cu,Zn)_5(CO_3)_2(OH)_6$] [11,16–18]. Accordingly, CuO, ZnO and an amorphous phase, probably containing a mixture of oxides, were observed on the X-ray diffraction profiles of the calcined catalysts [16,17]. No diffraction peaks belonging to the $CuAl_2O_4$ phase could detected.

Relatively high BET specific area and pore volume values were obtained for the calcined catalysts as compared to that of the commercial catalyst. These discrepancies seemed nevertheless reasonable, considering that the commercial catalyst was previously submitted to pelletizing and stabilization processes not applied for the laboratory synthesized samples.

Significant differences were found for the copper metallic surface area and copper dispersion values for catalysts prepared according to different precipitation sequences. The obtained values suggest that the phase interdispersion is affected by the precipitation sequence, allowing a better copper exposure when copper and zinc were simultaneously coprecipitated. Single phase or mixtures of Cu,Zn hydroxycarbonates are usually reported as resulting products of Cu and Zn coprecipitation [8,11,14,17,18], at experimental conditions similar to those used in this study. Thus, the addition of aluminum hydroxide to the Cu,Zn hydroxycarbonates precursor seemed to contribute to increase both the BET and the metallic copper surface area, as observed for catalyst CZ-A. The role of spacer or textural promoter has been commonly postulated for aluminum

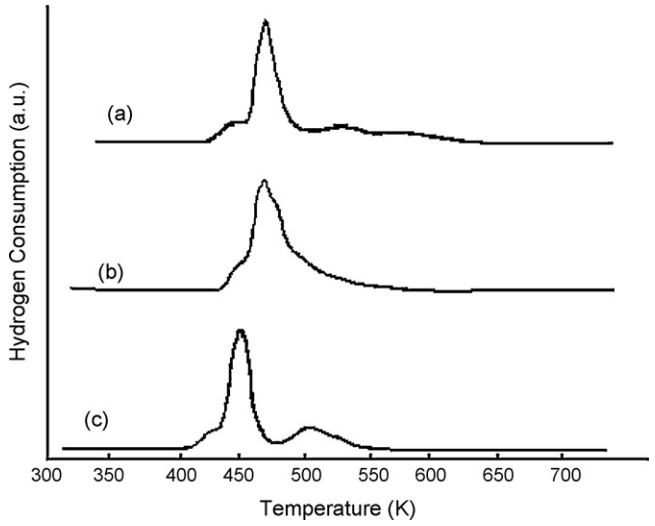

Fig. 1. Temperature-programmed reduction profiles for (a) CZA; (b) CZ-A; (c) CA-Z.

oxide either in the LT-WGSR or the LT-methanol synthesis catalysts [19]. On the other hand, it has been demonstrated using statistical design of experiments that ZnO plays a role of a dispersion agent for small copper clusters in active LT-WGSR catalysts [17].

The system under investigation consists of copper oxide, zinc oxide and alumina oxide where the last one is a minor constituent. The reactivity of the oxide is clearly an effect of the nature the oxide and probably depends on the crystallite structure within the individual particle. Properties such as Cu^{2+} dispersion on the oxide matrix, Cu^{2+} chemical environment, crystal size of CuO and degree of crystallization, among others, are key properties in determining reduction behavior. Therefore, TPR was a very valuable tool to detect alterations in the Cu^{2+} state in different samples.

Fig. 1 shows the reduction profile of the calcined catalysts between 373 and 573 K. Estimation of the extent of reduction from the integral of these curves revealed that copper oxide was stoichiometrically reduced to Cu^0. The catalyst reduction profiles presented in Fig. 1 show different profiles and peak positions. Considering that all the experiments were performed under the same experimental conditions, such differences were caused by changes in the chemical environment. The distribution of metallic particle size in the catalysts and the reduction behavior of calcined samples are due to not only the interaction between the Cu^{2+}, Zn^{2+} and Al^{2+} phases, but also to the dispersion of Cu^{2+} phases in the $ZnO–Al_2O_3$ matrix and CuO crystal size.

On the basis of slope changes, the TPR profiles given in Fig. 1 include three steps: (i) the reduction or H_2-consumption corresponding to a shoulder peak placed around 400–450 K can be mainly ascribed to a reduction of Cu^{2+} to Cu^{1+} and the rate is low. Considered that this step represents a surface reaction and postulated that the diffusion of anion vacancies away from the surface [17] into the interior of the solid, could be the rate determining step at this stage; (ii) the second step is characterized by a rapid increase in the reaction rate, while the main reduction process is apparently attributable to the reduction of Cu^{2+} and/or Cu^{1+} to Cu^0 within the temperature interval 450–500 K. Most of the reduction is completed at this step. It can be seen from the reduction curves (Fig. 1) that there is a progressive rise in the reduction rates with the temperature rise, suggesting that cupric oxide is directly reduced to copper without any intermediate lower oxides being formed; (iii) in the third step, the last step in the reduction profile presented in Fig. 1 occurs after the main reaction is over.

The broad TPR profiles recorded for CZA, CZ-A and CA-Z oxide precursors indicate superposition of two or three peaks. They can represent the ill-defined structures of copper oxide in these catalysts. It is clearly demonstrated that, as temperature increases, at least four Cu^{2+} species were reduced in the calcined $CuO–ZnO–Al_2O_3$ catalysts, which can be attributed to copper in the ZnO lattice, in amorphous Cu oxide phases, in crystalline CuO and Cu^{2+} in the Al_2O_3 phase.

Different profiles were obtained for each experiment. CZA reduction showed one peak and took place at about 475 K, similar to the CZ-A catalyst. The CA-Z catalyst showed a profile which is different from the others. In addition to the main peak at lower temperatures (475–500 K), this catalyst presented a wider shoulder at 400–475 K and another shoulder at 500–550 K. The reduction profile of CZ-A was very similar to that obtained for CZA. This suggested that in CZ-A, most of the copper ions are dispersed as CuO in the ZnO matrix, corresponding to the reduction peak at nearly 478 K. For the reduction of these species, Gusi et al. [20] found an activation energy similar to that for CuO and called them as “free” copper. Furthermore, the small peaks only appearing as shoulders at nearly 450 and 500 K, represent minor contributions to the reduction process of catalyst CZ-A. On the contrary, a small and broad but well-defined high temperature reduction peak was observed for catalyst CA-Z, at 480–530 K. This is in agreement with the low reactivity towards reduction hypothesized for Cu^{2+} species interacting with aluminum in Cu/Zn/Al oxide precursors [20]. An intermediate behavior towards reduction was observed for catalyst CZA, suggesting that the interaction between the catalysts components may be selectively favored by the coprecipitation sequence. According to the TPR analyses, it also seemed that only aluminum influenced the reduction behavior of the ternary LT-WGSR catalyst [20,21].

The chemical state and relative concentration of the components at the surface were obtained from X-ray photoelectron spectra recorded under a reduction–oxidation cycle. The respective Cu 2p core-level spectra are displayed (Figs. 2–4) and corresponding binding energies are collected in Table 2. The BE corresponds to the values reported elsewhere [12,17,22–26]. In addition, as a satellite line is observed at above ca. 9 eV of the principal Cu $2p_{3/2}$ and Cu $2p_{1/2}$ levels, which is the fingerprint of Cu^{2+} ions, it can be concluded that copper remains in the copper state Cu(II). When the catalysts were vacuum treated or reoxidized (steps I and III, respectively) two copper species were observed: one at 932.9 ± 0.1 corresponds to Cu^{2+} ions in CuO and another at 935.1 ± 0.1 eV is assigned to Cu^{2+} ions dispersed in the oxide matrix [12]. Sepulveda et al. [27] assigned this last peak to Cu^{2+} ions in the spinel environment of $CuAl_2O_4$. Although the pattern for this compound could not be found by XRD analyses of the calcined precursor, evidences have been shown by TPR that the reduction behavior of Cu^{2+} ions was influenced by the presence of an Al containing phase. One single peak at 932.4 ± 0.1 eV and the absence of the satellite structure are conclusive on the presence of Cu and/or Cu^+ and may be observed in the spectra of the reduced catalyst (steps II and IV). The significant decrease in the Cu/Zn ratios for the H_2-reduced catalysts was interpreted as a decrease in copper surface dispersion as a consequence of growing the metallic copper particles on the oxide matrix, namely, ZnO and Al_2O_3.

After reoxidation (step III), the amount of the former Cu^{2+} species at 932.9 ± 0.1 eV significantly increased with respect to step I for catalyst CZA but remained nearly constant for catalysts CZ-A and CA-Z. On the other hand, the Cu/Zn ratio increased but it was not completely restored to the values found for the fresh calcined catalysts. The Cu/Zn surface ratio decrease was higher for CA-Z than for CZA and CZ-A. The reduction–oxidation cycle was finally accomplished upon reducing the catalyst at 493 K in a H_2 flow for 1 h and the peak at 932.4 ± 0.1 eV (step IV) was restored. A significant decrease in the Cu/Zn surface ratio was nevertheless observed for CA-Z and CZA with respect to the values found after

Table 2
Surface analyses of the Cu/Zn/Al catalysts under a reduction–oxidation cycle.

Sample	Step	Cu $2p_{3/2}$	Zn $2p_{3/2}$	Al 2s	Cu/Zn	Al/Zn	Cu/Al
CZA	I	932.9 (63)					
		935.0 (37)	1022.2	119.4	0.611	0.229	2.67
	II	932.4	1022.2	119.5	0.449	0.237	1.89
	III	933.1 (81)					
		935.2 (19)	1022.2	119.4	0.509	0.201	2.53
	IV	932.4	1022.2	119.3	0.239	0.216	1.106
CZ-A	I	932.9 (87)					
		934.9 (13)	1022.2	119.4	0.661	0.112	5.90
	II	932.4	1022.2	119.5	0.386	0.089	4.34
	III	932.8 (86)					
		935.2 (14)	1022.2	119.4	0.569	0.105	5.42
	IV	932.4	1022.2	119.4	0.301	0.073	4.123
CA-Z	I	932.9 (83)					
		935.2 (17)	1022.2	119.4	0.724	0.117	6.199
	II	932.4	1022.2	119.5	0.391	0.098	3.99
	III	933.0 (80)					
		935.0 (20)	1022.2	119.4	0.436	0.091	4.79
	IV	932.3	1022.2	119.4	0.190	0.107	1.77

Step I: calcined catalyst; step II: catalysts were reduced in a H_2 flow for 1 h at 493 K; step III: catalysts were reoxidized in an air flow for 2 h at 673 K; step IV: catalysts were further reduced in a H_2 flow for 1 h at 493 K.

the first reduction of the catalysts. Again, the Al/Zn surface ratio was not significantly affected upon the oxidation–reduction cycle.

The results presented above suggest that catalyst CZ-A is more easily reconstructed than catalysts CA-Z and CZA, after reduction or oxidation treatments. Under conditions similar to those of LT-WGSR, namely, reducing atmosphere and 493 K, catalyst CZ-A shows high Cu/Zn surface ratio, even after reoxidation. On the contrary, for catalysts CZA and CA-Z, the Cu/Zn surface ratio decreased after exposure to either oxidant or reducing atmosphere.

3.2. Activity testing

The performance of the ternary Cu/Zn/Al catalysts for WGSR is shown in Fig. 5, as a function of the reaction temperature. An activity increase is observed up to nearly 513 K, when catalyst deactivation by copper sintering seemed to become significant. In addition, a more defined activity maximum was observed for catalyst CZ-A, suggesting that it was more sensitive than the others towards this effect. This behavior could be nevertheless expected as catalysts CZ-A showed very fine copper particles dispersed over the $ZnO–Al_2O_3$ matrix.

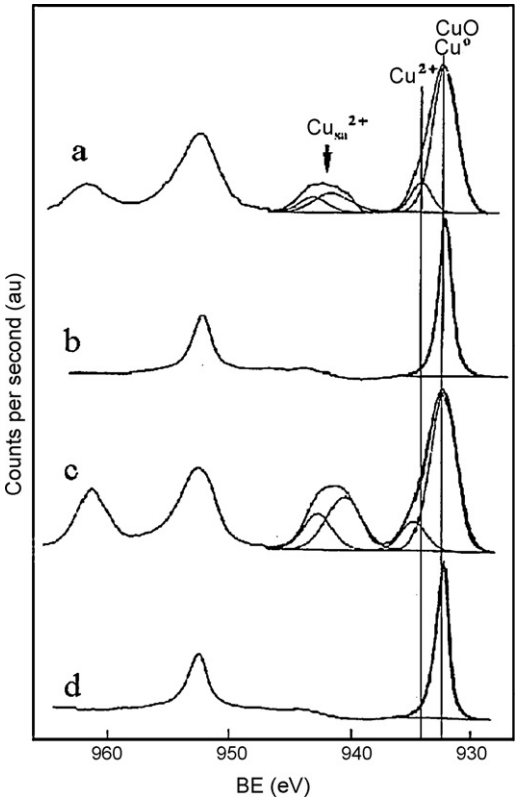

Fig. 2. Cu 2p core-level spectra for catalyst CZA: (a) calcined; (b) reduced at 493 K, for 1 h, in a H_2 flow; (c) reoxidized at 673 K, for 2 h, in an air flow; (d) reduced at 493 K, for 1 h in a H_2 flow, after reoxidation.

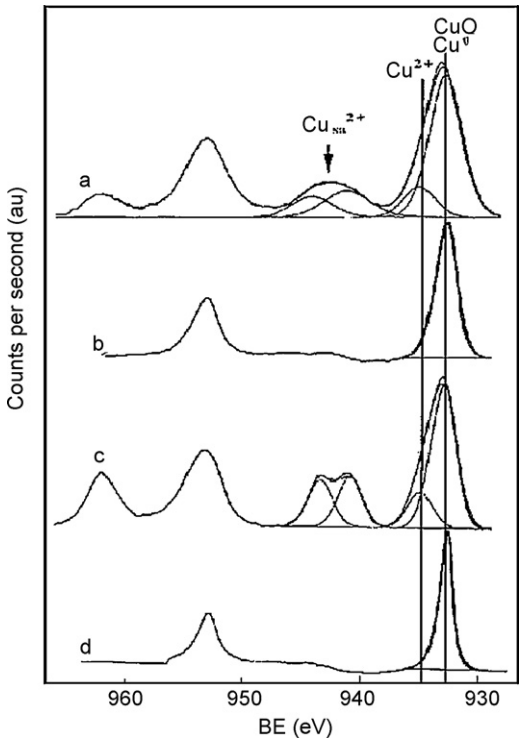

Fig. 3. Cu 2p core-level spectra for catalyst CZ-A: (a) calcined; (b) reduced at 493 K, for 1 h, in a H_2 flow; (c) reoxidized at 673 K, for 2 h, in an air flow; (d) reduced at 493 K, for 1 h in a H_2 flow, after reoxidation.

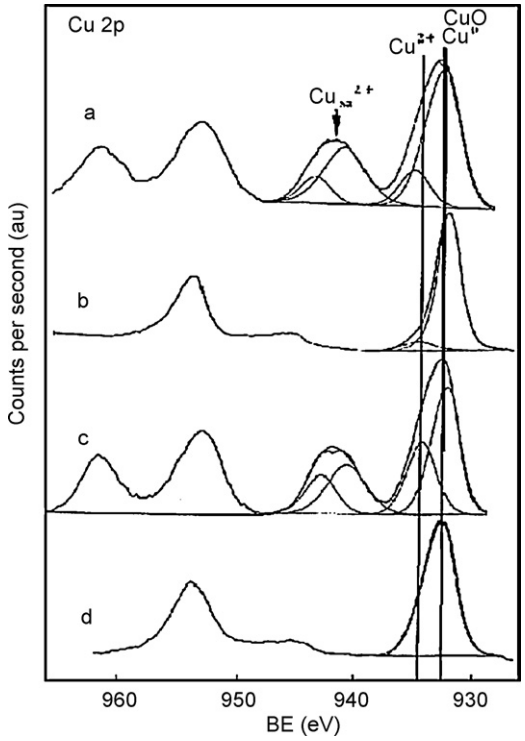

Fig. 4. Cu 2p core-level spectra for catalyst CA-Z: (a) calcined; (b) reduced at 493 K, for 1 h, in a H_2 flow; (c) reoxidized at 673 K, for 2 h, in an air flow; (d) reduced at 493 K, for 1 h in a H_2 flow, after reoxidation.

The stabilization of the catalysts under reaction conditions is shown in Fig. 6. Catalysts CZ-A and CA-Z quickly attained a stable activity but again CZ-A showed much higher activity than the other catalysts. The water gas shift reaction may be represented as:

$$CO(g) + H_2O(g) \Leftrightarrow CO_2(g) + H_2(g) \quad (1)$$

but side reactions such as:

$$CO(g) + 2H_2(g) \Leftrightarrow CH_3OH(g) \quad (2)$$

$$CO_2(g) + 3H_2(g) \Leftrightarrow CH_3OH(g) + H_2O(g) \quad (3)$$

may significantly contribute to the global process. The selectivity for reaction (1) is therefore strongly dependent on the steam/gas ratio molar, *V*/*G* [28].

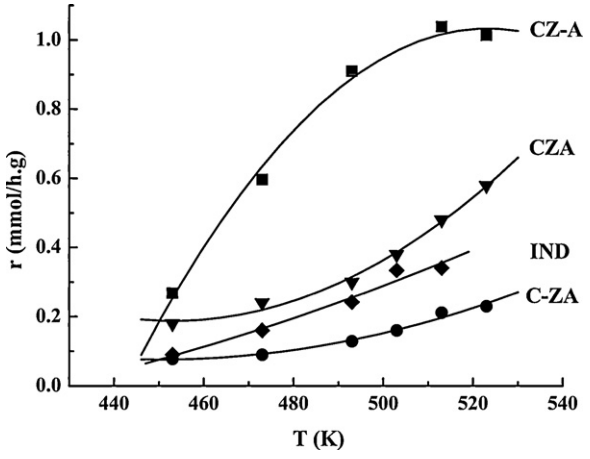

Fig. 5. Activity of the Cu/Zn/Al catalysts (mol CO converted per h and g of catalyst) as function of reaction temperature, at 493 K; *V*/*G* = 0.60; GHSV = 4500 h^{-1}.

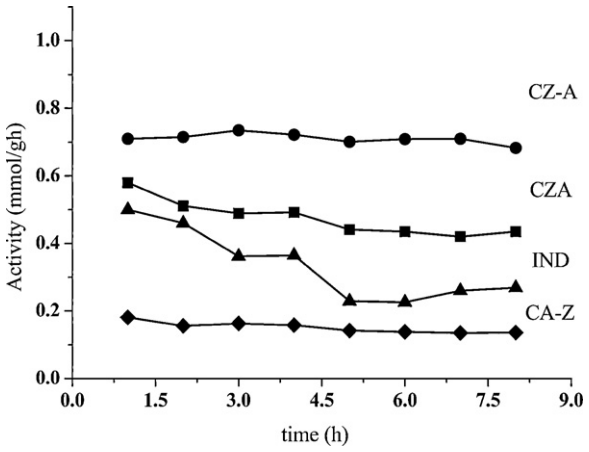

Fig. 6. Stabilization of the Cu/Zn/Al catalysts for WGSR, at 493 K, *V*/*G* = 0.60, and GHSV = 4500 h^{-1}.

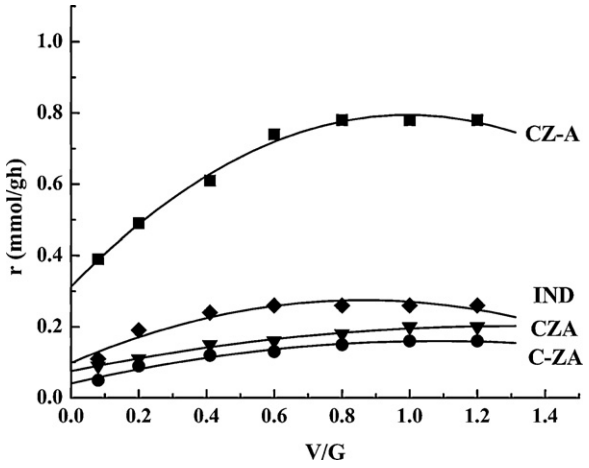

Fig. 7. Influence of the *V*/*G* molar ratio on the activity of the Cu/Zn/Al catalysts for WGSR, at 493 K, GHSV = 4500 h.

The influence of the *V*/*G* ratio on the activity towards the shift reaction is shown in Fig. 7. CZ-A catalyst shows higher activity than the other catalysts, over the investigated *V*/*G* ratio range, namely, 0.0–1.4. An activity increase was observed with increasing the *V*/*G* molar ratio but it seemed to be stabilized for values above 0.7. Notwithstanding this, at low water vapor pressures, methanol production is favored, either according reaction (2) or (3). These reactions consume hydrogen produced according to reaction (1) and contribute to decrease the hydrogen yield. The later behavior was observed for all the investigated catalyst samples.

4. Conclusions

On the basis of results derived from this study, the following conclusions can be drawn: (i) high catalytic activity was found for catalysts prepared by simultaneous coprecipitation of the Cu- and Zn-components, namely, catalysts CZA and CZ-A. However, as indicated by the Cu/Zn and Cu/Al surface atomic ratio determined by XPS, the copper surface concentration on catalyst CZ-A was less affected than on catalysts CZA and CA-Z, when subjected to a reduction–oxidation cycle. (ii) Among the investigated catalysts, CZ-A attained high and stable activity towards the LT-WGS reaction under a broad range of reaction conditions. This catalyst has been prepared by coprecipitation of Cu- and Zn-components followed by combination with the fresh precipitated Al-component. In addition, it showed a high copper metal area that seemed to be easily

reconstructed after oxidation and reduction treatments, according to the XPS analyses. (iii) The TPR profiles obtained for the ternary Cu/Zn/Al catalysts indicated the presence of different Cu(II) species and suggested that the amount and the behavior towards reduction of each copper species might be related to the interdispersion of the catalyst components. (iv) These last findings were interpreted as a consequence of the coprecipitation sequence in the preparation method, allowing the interactions between the catalyst components to be selectively established and favoring the production of catalysts showing well-defined properties.

Acknowledgments

The authors are grateful to FAPITEC-SE and CNPq for the grants and to FAFEN S.A. for the reaction facilities.

References

[1] L. Lloyd, D.E. Ridler, M.V. Twigg, in: M.V. Twigg (Ed.), Catalysts Handbook, 2nd ed., Wolfe, London, 1989, p. 283.
[2] M. Levent, Int. J. Hydrogen Energy 26 (2001) 551.
[3] S. Lim, J. Bae, K. Kim, Int. J. Hydrogen Energy 34 (2009) 870.
[4] A.L.C. Pereira, G.J.P. Berrocal, S.G. Marchetti, A.A. Alexilda, O. Souza, M.C. Rangel, J. Mol. Catal. A: Chem. 281 (1–2) (2008) 66.
[5] A.J. Elliot, R.A. Hadden, J. Tabatabali, K.C. Waugh, F.W. Zemicael, J. Catal. 157 (1995) 153.
[6] R.A. Hadden, P.J. Lambert, R. Ranson, Appl. Catal. A: Gen. 122 (1995) L1.
[7] T. Shishido, Y. Yamamoto, H. Morioka, K. Takehira, J. Mol. Catal. A: Chem. 268 (2007) 185.
[8] M.J.L. Ginés, N. Amadeo, M. Laborde, C.R. Apesteguía, Appl. Catal. A: Gen. 131 (1995) 283.
[9] G. Wu, Y. Sun, Y.-W. Li, H. Jiao, H.-W. Xiang, Y. Xu, J. Mol. Struct.: Theochem. 626 (2003) 287.
[10] Y. Zhang, Q. Sun, J. Deng, D. Wu, S. Chen, Appl. Catal. A: Gen. 158 (1997) 105.
[11] J.-L. Li, T. Inui, Appl. Catal. A: Gen. 137 (1996) 105.
[12] G. Petrini, F. Montino, A. Bossi, F. Garbassi, in: G. Poncelet, P. Grange, P.A. Jacobs (Eds.), Preparation of Catalysts III, Elsevier, Amsterdam, 1983, p. 735.
[13] M.G. Kalchev, A.A. Andreev, N.S. Zotov, Kinet. Catal. 36 (1995) 821.
[14] T.M. Yurieva, React. Kinet. Catal. Lett. 55 (1995) 513.
[15] C.D. Wagner, L.E. Davis, M.V. Zeller, J.A. Taylor, R.H. Raymond, L.H. Gale, Surf. Interface Anal. 3 (1981) 211.
[16] S. Fujita, A.M. Satriyo, G.C. Shen, N. Takezawa, Catal. Lett. 34 (1995) 85.
[17] A.A.G. Lima, E.L. Moreno, M.N. de Souza, H.M.C. Andrade, Appl. Catal. A: Gen. 171 (1998) 31.
[18] F. Cavani, F. Trifiró, A. Vaccari, Catal. Today 11 (1991) 1.
[19] T. Fujitani, M. Saito, T. Watanabe, Y. Kannai, T. Kakumoto, J. Nakamura, T. Uchijima, Chem. Lett. (1994) 1877.
[20] S. Gusi, F. Trifiró, A. Vaccari, React. Solids 2 (1986) 59.
[21] M.N. de Souza, MSc. Dissertation, Universidade Federal da Bahia - UFBA, 1985.
[22] B.R. Strohmeier, D.E. Leyden, R.S. Fiel, J.M. Hercules, J. Catal. 94 (1985) 514.
[23] Y. Okamoto, K. Fukino, S. Iamanaka, S. Teranishi, J. Phys. Chem. 87 (1983).
[24] F. Garbassi, G. Petrini, J. Catal. 90 (1984) 106.
[25] F. Garbassi, G. Petrini, J. Catal. 90 (1984) 113.
[26] I. Grohmann, B. Peplinski, W. Unger, Surf. Interface Anal. 19 (1992) 591.
[27] A. Sepulveda, C. Márquez, I. Rodriguez-Ramos, A. Guerrero-Ruiz, J.L.G. Fierro, Surf. Interface Anal. 20 (1993) 1067.
[28] G. Ghiotti, F. Boccuzzi, Catal. Rev. Eng. Sci. 29 (1987) 151.